Performance, combustion and emission characteristics on VCR multi-fuel engine running on methyl esters of rubber seed oil

S. Murugapoopathi[1] · D. Vasudevan[1]

Abstract

This research work is proposed to test and evaluate the performance, combustion and emission characteristics of variable compression ratio engine fueled with methyl esters of rubber seed oil as biodiesel. Experiments are carried out on variable compression ratio engine by considering the compression ratio, load, fuel blends, injection pressure and supercharging pressure as variables. The response surface method prediction models for indicated mean effective pressure, brake thermal efficiency, specific fuel consumption, exhaust gas temperature, maximum combustion pressure, heat release rate, ignition delay, carbon monoxide, hydrocarbon and nitrogen oxides emission are developed using the experimental results. D-optimality test is carried out to get optimum engine-operating conditions with improved performance and emission. Test is conducted via the fuel blends of 20, 40, 60 and 80% biodiesel with neat diesel, with an injection pressure of 160 bar at a fixed compression ratio of 20 and at different supercharging conditions at 80% load. The results of the experiment are compared with that of diesel, which confirms that significant improvements in performance and emission characteristics are obtained with the help of supercharging. The combustion characteristics of biodiesel blends comprehend with that of standard diesel.

Abbreviations

VCR	Variable compression ratio
MRSO	Methyl esters of rubber seed oil
IP	Injection pressure (bar)
CR	Compression ratio
BTE	Brake thermal efficiency (%)
BSFC	Brake specific fuel consumption (kg kW^{-1} h^{-1})
RSO	Rubber seed oil
ID	Ignition delay (°CA)
SC	Supercharging
NA	Naturally aspirated
HRR	Heat release rate (J °CA^{-1})
IMEP	Indicated mean effective pressure (bar)
EGT	Exhaust gas temperature (°C)
CA	Crank angle
CO	Carbon monoxide (%)
CO$_2$	Carbon dioxide (%)
HC	Hydrocarbon (ppm)
NO$_x$	Oxides of nitrogen (ppm)
IS	Indian standards
RSM	Response surface methodology
ANOVA	Analysis of variance
ASTM	American society of testing and materials
bTDC	Before top dead center
FFA	Free fatty acid
p test	Probability test
F test	Fisher's test
B20	20% biodiesel + 80% diesel
B40	40% biodiesel + 60% diesel
B60	60% biodiesel + 40% diesel
B80	80% biodiesel + 20% diesel
B100	100% biodiesel

List of symbols

P_{max}	Combustion pressure (bar)
R^2	Coefficient of determination
adj	Adjusted
X	Test statistics

✉ S. Murugapoopathi
poopathism@gmail.com

[1] Department of Mechanical Engineering, PSNA College of Engineering and Technology, Dindigul 624622, India

σ Standard deviation
μ Mean
θ Crank angle
g Gauge pressure

Introduction

Biodiesel plays a prevailing role to replace conventional fuel with fuel that is eco-friendly in nature [1]. The performance and emission characteristics of biodiesel blended with diesel and alcohol are tested in diesel engine to analyze the suitability of fuel [2, 3]. Various researches proved that the biodiesel and vegetable oils reduce the emission with its equivalent performance with diesel fuel [4, 5]. Biodiesels produced from non-food crop are promising fuels compared to that of diesel with minimum cost [6]. Transesterification is the process of improving the fuel properties of vegetable oils and the blend of vegetable oil with the addition of butanol and neat diesel characteristics which are comparable with that of diesel fuel [7]. A review was conducted on performance, combustion and emission characteristics of various fuels derived from oil seeds to promote alternate fuels to improve rural economy. The reports revealed that the biodiesel emission of various oil seeds of NO_x is higher than diesel, whereas CO, HC and CO_2 emissions are comparable with that of diesel [8]. Depletion of fossil fuel and increase in fuel price exaggerate the need for alternate sources. The fuel properties of methyl esters of rubber seed oil blended with diesel (B10 & B20) are tested in laboratory which accomplishes the ASTM standard of biodiesel [9]. Biodiesel produced from unrefined rubber seed oil needs two-step transesterification to reduce FFA content of the oil below 2%. The properties are compared with diesel and comprehend with the relative performance of the oil as alternative fuel [10]. Limestone-based catalyst obtained from cement clinker employed in this process converts rubber seed oil into biodiesel with high conversion efficiency [11]. The methyl esters of rubber seed oil produced using two-step transesterification process is tested in diesel engine with different blends of biodiesel with diesel. The blend B5 gives significant improvements in performance and reduction in emission compared to that of diesel without engine modification [12]. The performance and emission characteristics of rubber seed oil-based biodiesel are tested in diesel engine. The reported results show that the blends of biodiesel with 50–80% give brake thermal efficiency with acceptable values and more carbon deposits found in case if rubber seed oil needs to be investigated without any operational difficulties and engine modifications [13]. The performance and emission of rubber seed oil-derived biodiesel is tested in diesel engine, whereas B20 and B60 have lower smoke emission and comparable CO and HC emission, comprehending with that of diesel. The properties of rubber seed oil are close to diesel, and it can be partially replaced up to 60% [14]. The performance of rubber seed oil is improved by injection of diethyl ether at different proportions, and the results are compared with neat biodiesel and diesel. The injection of diethyl ether with biodiesel reduces HC and CO emissions with the combustion enhancement. The NO_x emissions of diethyl ether with RSO increase compared to biodiesel but lower than diesel due to premixed combustion phase [15]. The performance of cotton seed oil with recommended injection pressure under supercharged condition reduces the BSFC by 15% at full load and smoke density compared to diesel mode. Raising IP does not contribute to any improvements in engine performance while the engine is operated on both diesel and cotton seed oil [16]. Palm stearin methyl ester blended with diesel and ethanol at 20 and 30% of fuel blends with supercharging improves the BTE, and reduction in BSFC is observed. But the emission of CO, HC and NO is slightly increased with supercharging compared to naturally aspirated engine for same fuel blends [17]. The performance and emission characteristics of diesel engine are tested for different compression ratios (15:1 & 18:1), engine loads (25%, 50%, 75% & 100%) and biodiesel blends (10% & 20%). There is an increase in BTE about 31% observed with a reduction in BSFC for ethyl esters of B10 with increase in CR as compared to diesel. CO and HC emissions decrease; and at the same time, CO_2 and NO_x emissions increased with rise in CR [18]. The increase in stroke volume of the diesel engine increases the power output, which in turn increases the thermal efficiency to maximum at optimum compression ratio [19]. The optimum compression ratio identified with numerical study, by varying compression ratio and pressure ratio at its maximum pressure, attains maximum thermal efficiency with its minimum entropy generation for dual cycle [20]. The response surface methodology-based numerical model is developed to evaluate the performance and emission of diesel engine by varying compression ratios and fuel blends. The results revealed that the rise in CR helped to decrease the HC and CO emissions, but it increases the CO_2 and NO_x emissions. The BTE is better in the case of lower blends (B10) with lesser fuel consumption observed for the same engine setting [21]. The desirability-based optimization is used to maximize the performance and minimize the emission of VCR engine using RSM. The validated results revealed that the significant improvement in its performance and least emissions are observed with lower blends of biodiesel compared to that of diesel [22].

From the literature survey, most of the researchers conducted the performance and emission studies for compression ratio range of 16.5:1 to 18.5:1 with the varying loads, blends and speeds [18]. Also, very few studies

revealed the effect of supercharging in the VCR engine on the performance and emission parameters [16]. In this work, the optimum performance of methyl esters of rubber seed oil with neat diesel is extensively studied by varying compression ratios from 18:1 to 22:1 at different loads. The different blends of biodiesel are tested in variable compression ratio engine with and without supercharging at optimum injection pressure. The performance and emission characteristics of biodiesel are observed and compared with that of standard diesel with and without supercharging at fixed compression ratio. The combustion characteristics such as combustion pressure, heat release rate and ignition delay are discussed at various crank angle positions by varying supercharging conditions.

Materials and methods

Preparation and testing of biodiesel

In India, rubber (*Hevea brasiliensis*) tree is cultivated for the production of latex but the seed is left unused. This non-edible, transesterified rubber seed oil (RSO) extracted from the rubber seed is blended with diesel to produce biodiesel blends. The free fatty acid content of RSO is above 2%, needs two-step transesterification process, and its fatty acid composition is presented in Table 1. In transesterification process, each liter of RSO is mixed with 200 mL of methanol and 6 mL of sulfuric acid. The mixture is heated to 50 °C for acid esterification process and allowed to settle down for 10–12 h. End of the settling process, the impurities floating at the top are removed. Subsequently, the oil is again heated to 55 °C. In alkaline esterification process, 4 g of potassium hydroxide is added, in which dissolved 300 mL of methanol is mixed with oil and is stirred using magnetic stirrer for one hour. Methyl esters of rubber seed oil are settled in upper layer and are removed and heated about 80 °C to remove the moisture in the fuel. The fuel properties such as viscosity, density, flash point, fire point, calorific value and cetane index are tested

in the laboratory as per ASTM/IS1448 standard [23]. The outcome of biodiesel and its blends are to comprehend with the accepted limits [24] and are tabulated in Table 2.

## Experimental investigation on VCR engine

The experimental setup consists of a single-cylinder, water-cooled, four-stroke, direct injection, VCR engine, an eddy current dynamometer, an exhaust gas analyzer, a fuel flow meter, and air flow meter, a speed sensor, an exhaust gas calorimeter and a data acquisition system with personal computer (Fig. 1). The engine specifications are presented in Table 3. The performance analysis is performed using "Engine Test Express V8.5" software. The emission parameters are measured with Mars Technologies five gas analyzer. All sensors and loading devices are calibrated before taking the readings. The accuracy and sensitivity of measurement are described in Table 4. Initially, the engine is run at 1500 rpm with diesel for 6–8 h continuously to achieve steady state at different loads. The experiment variables are the load, compression ratio, fuel blends, injection pressure and supercharging pressure. The biodiesel blends are prepared as 20, 40, 60 and 80% with diesel on volume basis for different compression ratios. In this experiment, the injection pressure is varied from 140 bar, 150 bar and 160 bar and by varying supercharging pressures of 0, 0.25 and 0.5 bar gauge pressure, respectively, measured at inlet manifold. The experiment is conducted to analyze the performance, combustion and emission characteristics of VCR engine with supercharging and is compared with naturally aspirated engine. Once the engine gets warmed up, the emission and combustion observations are recorded for 100 cycles per minute [25] and cycle-to-cycle variation is averaged.

RSM-based prediction model

The input variables are sometimes called independent variables, and they are subjected to the control of the experiments. The response surface methodology is based on the experimental strategy for exploring the space of the process or independent variables, empirical statistical modeling to develop an appropriate approximating relationship between the yield and the process variables. Also, the optimization provides the method for finding the values of the process variables that produce desirable values of the response. RSM uses various statistical, graphical and mathematical techniques to develop the mathematical model and to analyze the problem by creating the relationship between one or more responses and a set of input variables. It is an efficient method of capturing information from available data gathered through physical experiments. This method is used to effectively explore the set of all

Table 1 Free fatty acid composition of rubber seed oil[a]

Fatty acid	Structure	Formula	Composition/mass%[a]
Palmitic acid	C16:0	$C_{16}H_{32}O_2$	10.2
Stearic acid	C18:0	$C_{18}H_{36}O_2$	8.7
Oleic acid	C18:1	$C_{18}H_{34}O_2$	24.6
Linoleic acid	C18:2	$C_{18}H_{32}O_2$	39.6
Linoleic acid	C18:3	$C_{18}H_{30}O_2$	16.3

[a][8]

Table 2 Properties and Indian standards of biodiesel and diesel

Properties	Diesel	B20	B40	B60	B80	B100	Biodiesel standards[a,b]	
							ASTM D 6751-02	IS 1448/DIN EN 14214
Density/kg m^{-3}	0.835	0.82	0.86	0.87	0.88	0.89	–	0.86–0.90
Viscosity at 40 °C/mm^2 s^{-1}	1.382	0.643	1.032	1.45	2.24	3.42	1.9–6.0	3.5–5.0
Flash point	42/°C	50/°C	56/°C	65/°C	120/°C	210/°C	> 130	> 120
Fire point	65/°C	54/°C	60/°C	75/°C	160/°C	230/°C	–	–
Calculated cetane index	45–55[c]	49	47	45	41	39	41 min	51 min
Gross calorific value/kJ kg^{-1}	45200[c]	41343	40200	39129	38070	36986	–	–

[a][24]

[b][29]

[c][31]
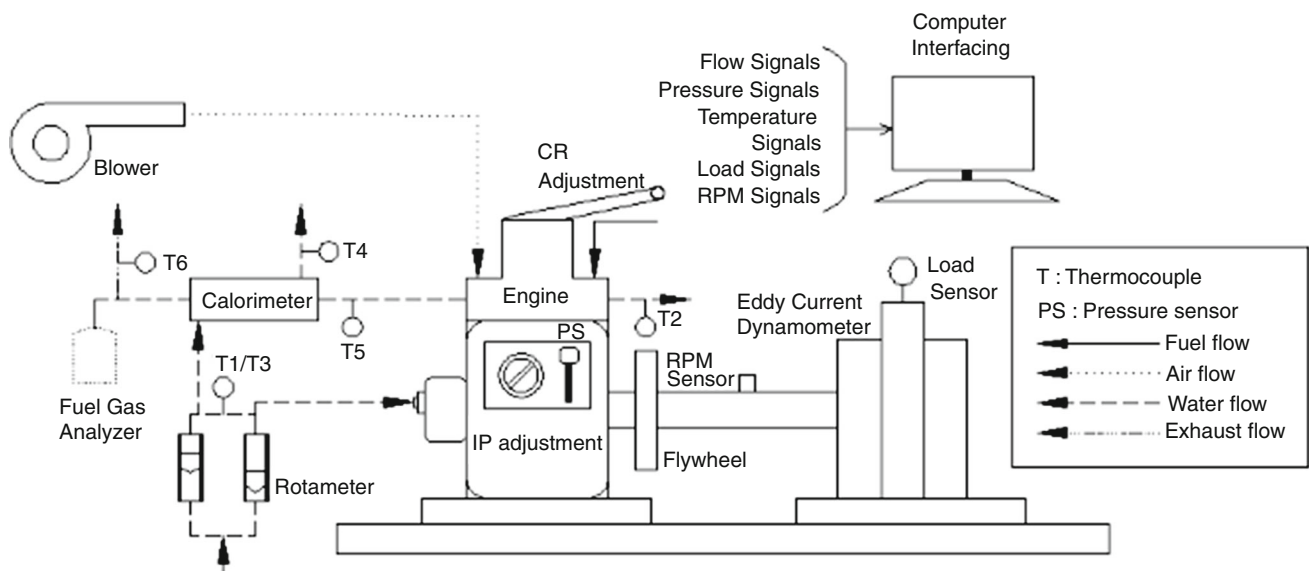
Fig. 1 Schematic diagram of the experimental setup

Table 3 Specifications of the variable compression ratio engine

General details	4-stroke, water-cooled, variable compression ratio engine, direct injection
Rated power	3.7/kW
Speed	1500 Rpm (constant)
Number of cylinders	One
Compression ratio	5:1 to 22:1 (variable)
Bore	80/mm
Stroke	110/mm
Ignition	Compression ignition
Loading	Eddy current dynamometer
Load sensor	Strain gauge load cell

possible combinations of variables that are tested when the total design space is large. The RSM is also used to develop simulation or physical model when the resources are very limited. The RSM model to be developed should be in the form of the following two-degree polynomial Eq. (1).

$$y = \beta_0 + \sum_{i=1}^{k} \beta_i X_i + \sum \sum_{i<j} \beta_{ij} X_i X_j + \sum_{i=1}^{k} \beta_{ij} X_i^2 + \varepsilon \quad (1)$$

where β is regression coefficient, k is the number of factor, i is the linear coefficient, j is the quadratic coefficient, y is the response and ε is the random error, $X_1, X_2, \ldots X_k$ are the input parameters.

The experimental results are used as the input for the RSM to develop an empirical model such that the CR, load, blend, IP and supercharging pressure are the variables and

Table 4 Uncertainty in measurement

Measurements	Accuracy
Engine speed	$\pm$ 5/rpm
Time	$\pm$ 0.20/%
Specific fuel consumption	$\pm$ 1/%
Temperature	$\pm$ 2/°C
Crank angle encoder	$\pm$ 0.5/°CA
Piezoelectric sensor	$\pm$ 0.50/%
Carbon monoxide	0.02/%
Hydrocarbon	0.05/%
Carbon dioxide	0.5/ppm
Nitrogen oxides	0.5/ppm

the BTE, BSFC, IMEP, exhaust gas temperature, maximum pressure, ignition delay, CO, HC, CO_2 and NO_x emissions are the response factors. The engine-operating parameters are also optimized through RSM for the better performance and emission results, and the same is verified experimentally. The objective of the study is to evaluate the VCR engine performance to optimize the CR and blend using RSM with help of supercharging. RSM tool is used to reduce the number of reputations in experimental design and reduces time and cost of experiments without compromising the engine calibration.

Analysis of variance (ANOVA) is used to evaluate whether the model has a strong influence on the responses among the data. To fit the coefficients with objective function relationship, it requires the relationship between factors and responses with 95% confidence level. The p value obtained from the ANOVA is presented in Table 5. The quadratic equation is weighed with R^2 value, which determines whether the model is deemed to fit. The value of R^2 and adj.R^2 near to one are desirable to verify the model adequacy with the required response. The p-test value obtained from the model evaluation should be less than 0.05 to accept the factors and responses which are to be significant.

Model testing and analysis

The model is evaluated using analysis of variance (ANOVA) to verify the model fitness and adequacy. There are 32 runs evaluated, and the normal probability is confirmed with the runs from the experiment. The responses of the model are significant with p-values and are less than 0.05. The agreement of R^2 with adj.R^2 is also close to each other to fit the quadratic model with the experimental results. The R^2 value is used to check the closeness of statistical data to fit the regression line by minimizing the

variance between the data points. The better linear regression fits the data points than the averaged one proposed by Cox and Snell [26] in Eq. (2)

$$R^2 = 1 - \left(\frac{L(0)}{L(\hat{\theta})} \right)^{2/n} \tag{2}$$

where $L(0)$ likelihood intercepts model; $L(\theta)$ estimated model and n the sample size.

The numerical model developed using RSM has a good agreement with its responses. The predicted results are validated and compared with the experimental results, and they are close to each other as shown in Table 6. The maximum error is found to be less than 5% for all the response functions except HC emission which is 15.9% error. The polynomial model developed for VCR engine can be utilized to find the optimum experimental values by varying the input factors at reduced time and cost.

Validation of optimized parameter

The desirability-based optimal test was conducted to find the correlation between factors and responses. The D-optimality quadratic model [27] was proposed to find solution for large set of observations in Eqs. (3) and (4).

$$Y = X * B + e \tag{3}$$

where Y experimental observations; e vector of errors; B tuning parameters in vectors.

$$Y = (X^T * X)^{-1} X^T Y \tag{4}$$

D-optimality test in this experimentation reduced the maximum variance of the predicted responses associated with the numerical model which in turn minimizes the error in experiments in terms of coefficient response model. The effect of compression ratio, load, supercharging and biodiesel blends had impact with composite desirability on all responses. There is a decline in all responses perceived when the biodiesel content in the blend increased, and the BSFC is also increased. It is observed that the rise in injection pressure to 160 bar resulted in an optimum performance in all aspects except ignition delay [28]. The optimum results are also obtained at the supercharging pressure of 0.25 bar (g) except IMEP due to its increase in CR. The combined desirability sets close to 1 fits the objective function with its parameters and responses. The desirability test is carried out by assigning suitable lower and upper limits for each factor and their responses with a weightage of 0.1 to 1. There is a suitable goal and importance committed to each response based on its weightage presented in Table 7. The combined desirability obtained for overall response is found to be 0.98548.

Table 5 Experimental design matrix

Run order	A (CR)	B (load—kg)	C (blends—%)	D (IP—bar)	E (SC pressure—bar (g))	IMEP/bar	BTE/%	BSFC/kg/kWh	P_{max}/bar	ID/°CA	CO/%	HC/ppm	NO_x/ppm	Exhaust temp/°C
1	20	8	40	150	0.5	8.54	35.67	0.26	70.35	12.20	0.25	9	391	285.34
2	20	8	0	150	0.25	8.89	36.10	0.20	65.98	11.82	0.18	19	542	225.63
3	22	4	40	140	0.25	5.97	24.75	0.40	71.80	11.82	0.29	14	306	211.36
4	20	8	40	160	0.25	8.14	34.70	0.30	67.80	11.60	0.22	10	333	283.32
5	20	4	80	160	0.25	5.14	17.52	0.69	65.48	11.82	0.20	9	217	232.93
6	18	4	40	140	0.25	5.09	26.11	0.40	61.41	11.94	0.28	9	310	223.53
7	20	4	40	150	0.25	4.73	23.47	0.38	67.66	11.81	0.13	15	222	216.40
8	18	8	40	150	0.25	8.33	37.93	0.25	61.82	11.95	0.29	9	453	284.48
9	20	4	40	150	0.25	4.73	23.47	0.38	67.66	11.81	0.13	15	223	216.40
10	22	0	40	150	0.25	1.75	0.00	0.00	67.82	11.89	0.20	9	240	212.85
11	22	4	40	150	0	5.13	17.83	0.39	67.51	11.63	0.31	12	332	226.69
12	20	4	80	140	0.25	5.09	17.81	0.63	65.99	11.92	0.27	11	285	229.65
13	22	4	40	160	0.25	5.23	23.81	0.53	71.03	11.80	0.27	9	265	219.63
14	20	8	40	140	0.25	8.77	34.79	0.30	68.20	12.20	0.28	10	483	289.63
15	20	0	80	150	0.25	1.58	0.00	0.00	62.42	11.76	0.19	15	236	216.44
16	20	0	40	160	0.25	1.43	0.00	0.00	62.56	12.05	0.13	9	299	219.87
17	20	0	0	150	0.25	0.86	0.00	0.00	60.33	11.90	0.08	11	151	165.90
18	18	4	40	150	0	4.85	26.31	0.34	58.82	11.76	0.24	8	298	226.98
19	20	0	40	140	0.25	1.46	0.00	0.00	62.06	11.67	0.14	10	155	217.52
20	20	4	0	150	0.5	4.66	24.70	0.35	62.08	11.78	0.11	8	357	172.65
21	20	4	0	160	0.25	4.85	24.94	0.37	63.82	11.84	0.12	14	298	166.96
22	20	4	40	160	0.5	5.03	25.07	0.40	64.73	11.90	0.17	11	263	232.54
23	20	4	80	150	0.5	5.34	18.54	0.58	67.59	11.90	0.20	10	163	228.65
24	20	4	80	150	0	5.02	17.43	0.59	61.99	11.69	0.26	6	343	243.69
25	22	4	0	150	0.25	5.00	24.23	0.32	67.99	11.71	0.18	4	372	152.69
26	18	4	0	150	0.25	4.74	23.80	0.39	59.00	11.90	0.23	30	284	172.59
27	20	4	40	160	0	5.97	25.93	0.39	64.20	11.72	0.15	1	244	239.87
28	22	4	80	150	0.25	5.61	14.14	0.69	71.93	11.85	0.38	29	230	226.98
29	20	0	40	150	0	1.27	0.00	0.00	61.95	12.08	0.17	9	220	231.58
30	20	0	40	150	0.5	2.60	0.00	0.00	59.00	11.45	0.09	6	156	215.11
31	20	4	40	150	0.25	4.73	23.47	0.38	67.66	11.81	0.13	15	222	179.86
32	20	4	0	150	0	4.60	23.50	0.35	62.42	11.83	0.11	15	296	175.97

Table 6 Model evaluations

Model	IMEP/bar	BTE/%	BSFC/kg kWh^{-1}	Exhaust gas temp/°C	P_{max}/bar	ID/°CA	CO/%	HC/ppm	NO_x/ppm
p-value	< 0.0001	< 0.0001	< 0.0001	0.0001	< 0.002	< 0.0001	< 0.0001	0.0001	0.0002
SD	2.2249	11.052	0.18707	34.286	4.0941	0.15279	0.07373	5.6714	87.533
Mean	5.0738	21.052	0.33236	223.35	65.01	11.817	0.20371	11.342	284.31
R^2	0.9868	0.9888	0.9852	0.9772	0.9953	0.9956	0.9992	0.9963	0.9866
Adj. R^2	0.9763	0.9798	0.9734	0.959	0.9915	0.992	0.9986	0.9933	0.9758

The experimental results are validated with its predicted values of each response. The error is found to be less than 10% for each response except HC emission. The best value of BTE is found for blend MRSO20 at a compression ratio of 20 with 80% load, which is 3.73% higher than predicted value and maximum combustion pressure is 1.34% lower than the predicted value. The emission of CO and NO_x is found to be acceptable with less than 5% error and is due to variation in air flow condition and poor atomization of fuel. The optimum solution obtained using optimality test is presented in Table 8, and the same is validated with its predicted values in Table 9.

Results and discussion

The coefficient of variance (COV) for all parameters is calculated using the recorded experimental data of cycle-to-cycle variation for 100 cycles per min. expressed as [25],

$$COV = \frac{\sigma}{\mu} \times 100 \qquad (5)$$

where $\mu = \sum_{i=1}^{N} x_i / N$ and standard deviation (σ)

$$\sigma = \sqrt{\frac{1}{N} \sum_{i=1}^{N} (x_i - \mu)^2} \qquad (6)$$

The engine-operating parameters such as air flow rate, fuel flow rate, speed, inlet supercharging pressure and load play a major role in combustion characteristics such as heat release rate, combustion pressure, crank angle variation and cylinder gas temperature, which are analyzed at different operating conditions and discussed below. The performance, combustion and emission characteristics of VCR engine are conducted for identified optimum compression ratio of 20 with 80% load at a nozzle injection pressure of 160 bar for all blends with and without supercharging. The performance analysis is carried out to increase the thermal efficiency of the engine without compromising the emission; efforts are made to decrease the emission considerably using supercharging, CR and biodiesel blends. The combustion characteristics of VCR engine are analyzed suitably to optimize the maximum pressure and ignition delay with its input parameters. The emission characteristics such as HC and CO are reduced significantly with supercharging.

Performance characteristics

Brake thermal efficiency (BTE)

An increase in compression ratio increases the efficiency of lower blends up to MRSO40; afterward, there is a drop in efficiency due to its lower heating value and poor atomization of fuel [13]. The load, supercharging and blends are playing a major role in performance because the increase in load with sufficient air enhances the combustion at optimum pressure and CR. There is a definite change in brake thermal efficiency with supercharging as presented in Fig. 2. The maximum efficiency obtained at CR 20, MRSO20 with 0.25 bar (g) pressure, is 39.85% at 80% load

Table 7 Optimization criteria for responses of performance, combustion and emissions

Source	Lower limits	Upper limits	Weightage		Importance	Goal	Desirability
			Lower	Upper			
Compression ratio	18	22	1	1	3	In range	1
Load	0	8	1	1	3	In range	1
Biodiesel blends	0	80	1	1	3	In range	1
IP/bar	140	160	1	1	3	In range	1
SC pressure/bar(g)	0	0.5	1	1	3	In range	1
IMEP/bar	0.86	8.01	0.1	1	5	Maximize	0.9568
BTE/%	24.14	35.67	0.1	1	5	Maximize	0.9878
BSFC/Kg kWh^{-1}	0.38	0.69	1	0.1	5	Minimize	1
Exhaust gas temp./°C	225.63	293.67	1	0.1	5	Minimize	0.9632
P_{max}/bar	58.83	66.95	0.1	1	5	Maximize	0.9998
ID/°CA	11.40	12.20	0.1	1	5	Minimize	0.9617
CO/%	0.23	0.38	1	0.1	5	Minimize	1
HC/ppm	25	30	1	0.1	5	Minimize	1
NO_x/ppm	375	541	1	0.1	5	Minimize	1

Table 8 Optimized parameters

A—CR	B—load/kg	C—blend/%	D—IP/bar	E—SC pressure/bar(g)
20	8	20	160	0.25

Table 9 Validations of experiment

Optimized parameters					Value	IMEP/ bar	BTE/ %	BSFC/ kg kWh^{-1}	Exhaust gas temp/ °C	P_{max}/ bar	ID/ °CA	CO/%	HC/ ppm	NO$_x$/ ppm
A— CR	B— load/ kg	C— blends/ %	D— IP/ bar	E—SC pressure/ bar(g)										
20	8	20	160	0.25	Predicted	7.70	35.52	0.280	228.13	66.94	11.6	0.166	15	375
					Actual	7.62	36.90	0.26	232.24	66.06	11.3	0.172	13	385
					% Error	8.59	3.730	9.59	4.11	1.34	3.59	3.590	16	3
20	8	0	150	0.25	Predicted	8.82	35.28	0.23	223.49	65.54	11.4	0.181	19	536
					Actual	8.09	31.36	0.26	206.98	65.98	11.9	0.165	22	563
					% Error	9.04	12.51	11.50	7.98	0.67	4.15	9.700	14	5
20	8	40	150	0.25	Predicted	8.6	34.02	0.28	276.41	68.94	11.8	0.249	21	384
					Actual	8.09	32.96	0.27	294.11	69.24	11.9	0.283	25	437
					% Error	6.28	3.20	3.31	6.02	0.44	1.10	12.01	16	12

higher than diesel. The additional air supplied through blower enhances the combustion efficiency of biodiesel blends [24] at a compression ratio of 20. This is due to micro-flare up and better burning of fuel at 0.25 bar (g) pressure. For the same operating condition, the thermal efficiency is 36.57% and 37.71% for MRSO 20 observed with 0.5 bar (g) pressure and NA condition greater than diesel in all conditions. When biodiesel content increases in fuel blends, there is a drop in the efficiencies at NA engine due to lower calorific value and its poor volatility of biodiesel [17].
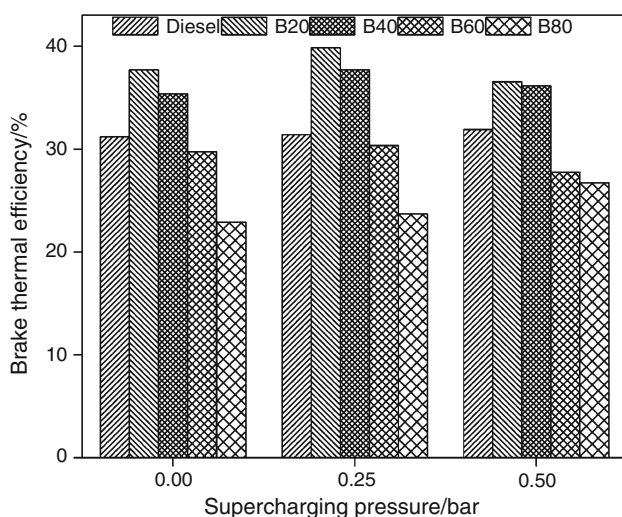
Fig. 2 Variations in brake thermal efficiency with supercharging for different blends at CR 20

Brake specific fuel consumption (BSFC)

Specific fuel consumption of VCR engine is subjected by various factors such as load, compression ratio, injection pressure and fuel quality. It is observed that the increase in biodiesel content in the fuel increases the fuel consumption due to its poor atomization of B80 at all conditions [24]. This can be overcome by increasing the CR, full load and injection pressure. But the shorter ignition delay of biodiesel increases the cylinder temperature at higher CR and at full-load operation [13]. There is a reduction in specific fuel consumption obtained with a blend of MRSO20 and MRSO 40 at CR 20 at 0.25 bar (g) pressure, which is 11.2% and 1.16% lower than diesel. The same trend is observed for blend MRSO20 and MRSO40 for 0.5 bar (g) pressure and NA condition shown in Fig. 3. The fuel consumption of higher blends is higher than diesel at all operating conditions due to its poor volatility and less fuel penetration depth at higher IP [16].

Indicated mean effective pressure (IMEP)

The average pressure acting on the piston indicated mean effective pressure. The IMEP depends on fuel quality and chemical reaction of fuel. There was an increase in IMEP at 0.5 bar (g) at compression ratio 20 due to its better mixing of fuel as shown in Fig. 4. The IMEP of diesel is comparable with that of MRSO40 and other blends at CR 20, with 0. 25 bar (g) pressure at 8 kg load compared to NA condition. In all the three supercharged conditions, the IMEP
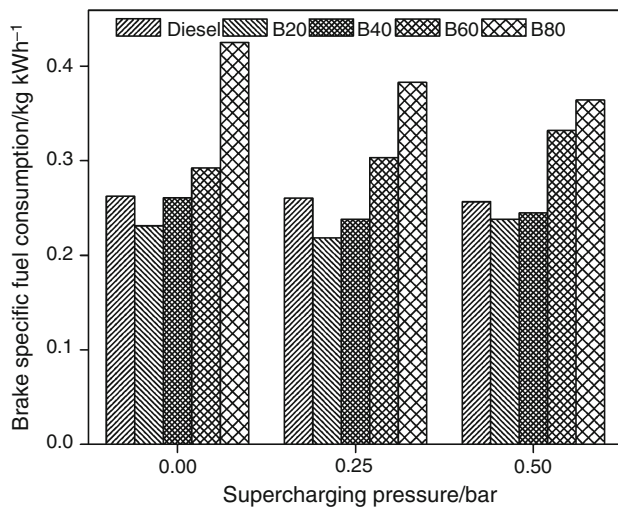
Fig. 3 Variations in brake specific fuel consumption with supercharging for different blends at CR 20

of B40 is closer to diesel due to its better lubricity at higher CR [29].

Exhaust gas temperature

Generally, biodiesel has shorter ignition delay, which reduces the time of combustion inside the cylinder at part and full-load operation. There is an increase in biodiesel content, which reduces the ignition delay of higher blends due to its oxygen content in the fuel [14]. There is a fall in exhaust gas temperature identified for its increase in biodiesel content due to its viscosity [13] as shown in Fig. 5. During the 80% load at CR 20, the maximum exhaust temperature of MRSO 60 and MRSO 80 was higher than diesel without supercharging, which reduces the physical

delay [30]. The increase in compression ratio and supercharging enhanced the combustion and reduced the effect of afterburning in exhaust manifold. The exhaust gas temperature decreases with increase in air flow variation at higher CR of blends [31] but higher than diesel due to its lower calorific value of the biodiesel. However, the heat lost to exhaust comprehends with the performance of the engine at higher CR [29].

Combustion characteristics

Combustion pressure (P_{max})

The combustion pressure with respect to crank angle is evaluated using energy equation [32] as follows:

$$\frac{dP}{d\theta} = \frac{k-1}{V}\frac{\partial Q}{\partial \theta} - k\frac{P}{V}\frac{dV}{d\theta} \tag{7}$$

where k specific heat ratio (c_p/c_v), P the pressure, V the volume, $\frac{dV}{d\theta}$ change in volume per °CA, $\frac{\partial Q}{\partial \theta}$ heat released gradient. The equation was solved by recording heat release gradient from experimentally per degree of crank angle rotation.

The instantaneous volume per degree CA for the given geometry of cylinder can be written from as [33],

$$V(\theta) = \frac{\pi D^2 L}{4(r-1)} + \frac{\pi D^2}{4}\frac{L}{2}(1-\cos\theta) + l\left[1 - \left\{\sqrt{1 - \left(\frac{L}{2l}\right)^2 \sin^2\theta}\right\}\right] \tag{8}$$

where D, L, l and r are the diameter, piston stroke, connecting rod length and compression ratio. Equation (5) was

Fig. 4 Variations in IMEP with supercharging for different blends at CR 20
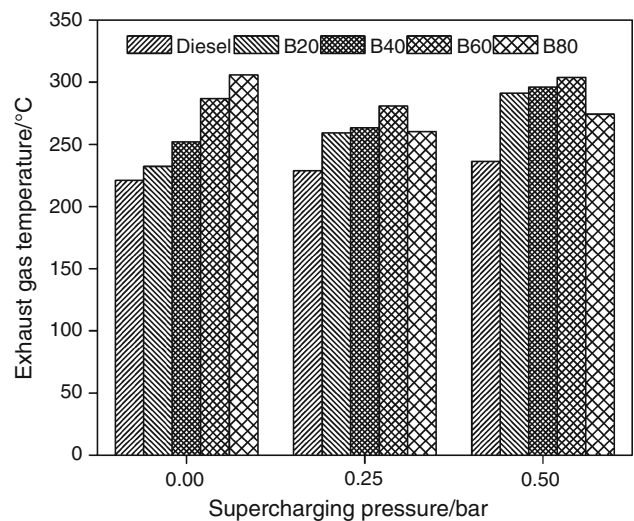
Fig. 5 Variations in EGT with supercharging for different blends at CR 20

solved by recording heat release gradient experimentally and $V(\theta)$ from analytical Eq. (6).

The combustion of VCR engine is improved by varying the CR, injection pressure, biodiesel blends and supercharging. The effect of increase in CR with supercharging pressure confirms good result of maximum combustion pressure as shown in Fig. 6. The rise in maximum pressure was obtained with CR 20 due to huge amount of fuel burned in premixed combustion [34]. The maximum pressure obtained without supercharging pressure at CR 20 of blends 20, 40, 60 and 80% and diesel is 65.21, 67.28, 67.88, 66.71 and 65.69 bar, respectively. The rise in compression ratio, oxygen present in the biodiesel and full load improve the combustion pressure compared to diesel [35].

It is revealed that the effect of supercharging at 0.25 bar (g) in diesel engine increases the maximum pressure presented in Fig. 7. The cylinder maximum pressure of blends 20,40,60 and 80% and diesel at 0.25 bar (g) supercharging at CR 20 is 69.92,67.42, 69.14, 71.44 and 70.7 bar, respectively. This is due to better mixing of air with fuel at premixed combustion phase with the rise in higher compression ratio. The power output of the engine increases with increase in stroke length up to optimum CR [19].

The combustion pressure of various biodiesel blends with supercharging pressure of 0.5 bar (g) is presented in Fig. 8. The maximum pressure obtained with various blends of 20, 40, 60 and 80% and diesel is 66.73, 67.01, 69.65, 67.7 and 67.04 bar, respectively. An increase in air supply at CR 20 reduces the maximum pressure compared to 0.25 (g) pressure and is performed better than naturally aspirated engine. The combustion of biodiesel depends on various factors such as heating value, air supply, ignition delay and fuel quality [31].
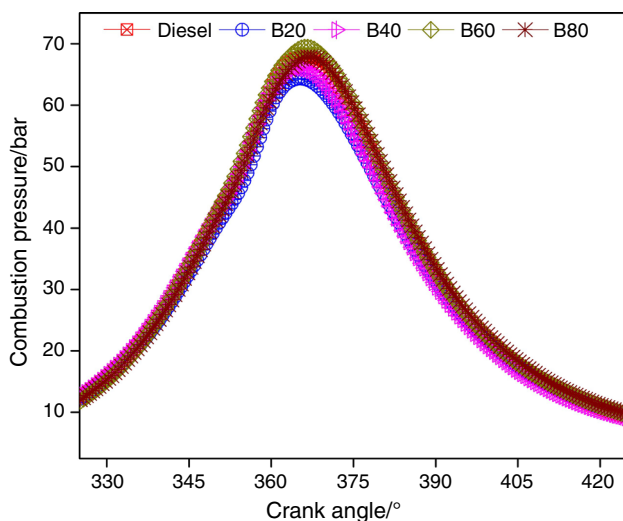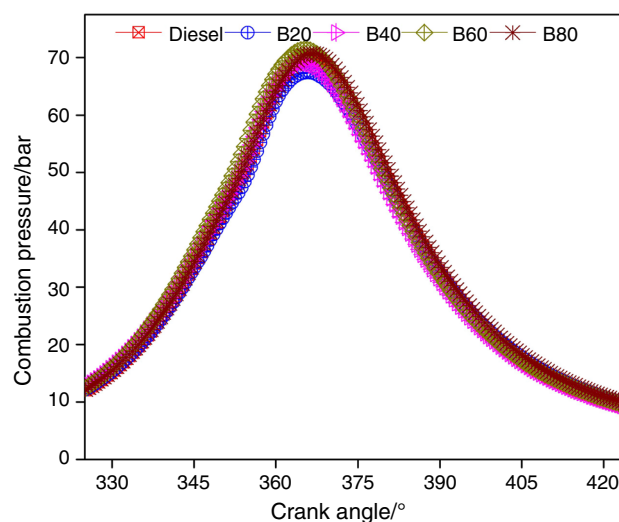
Fig. 7 Variations in combustion pressure with blends under supercharging of 0.25 bar (g) at CR 20

Heat release rate (HRR)

The heat release rate of naturally aspirated VCR engine with respect to crank angle is given in Fig. 9 for CR 20 at 80% load. The diffusion combustion of higher blends showed better trend with higher specific fuel consumption. The blend of B20 and B40 is slightly superior to that of diesel in NA condition. The heat release rate of blends is slightly higher than that of diesel and comparable with that of biodiesel at 0.25 bar (g) supercharging is shown in Fig. 10. The air entrainment at the start of fuel injection is overcome by supercharging of all fuel blends compared to diesel. Further increase in supercharging pressure to 0.5 bar gauge pressure slightly decreases the performance of biodiesel blends except that of diesel as shown in
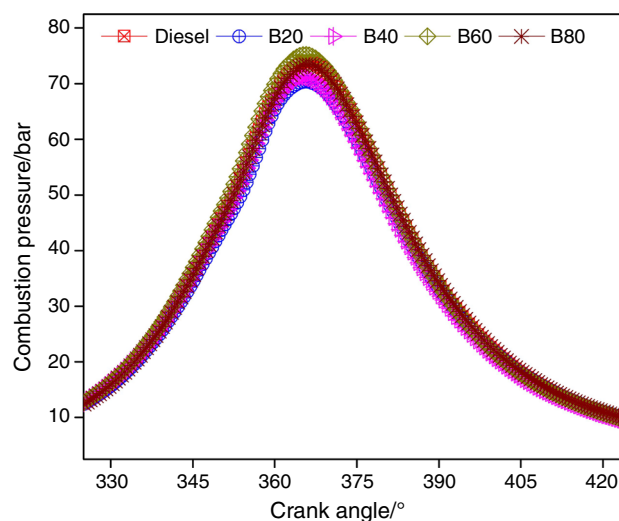

Fig. 6 Variations in combustion pressure with blends under NA condition at CR 20

Fig. 8 Variations in combustion pressure with blends under supercharging of 0. 5 bar (g) at CR 20
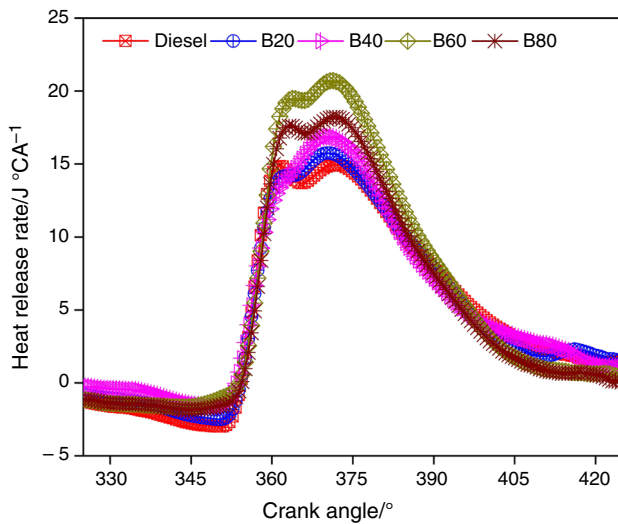
Fig. 9 Variations in heat release rate with blends under NA condition at CR 20
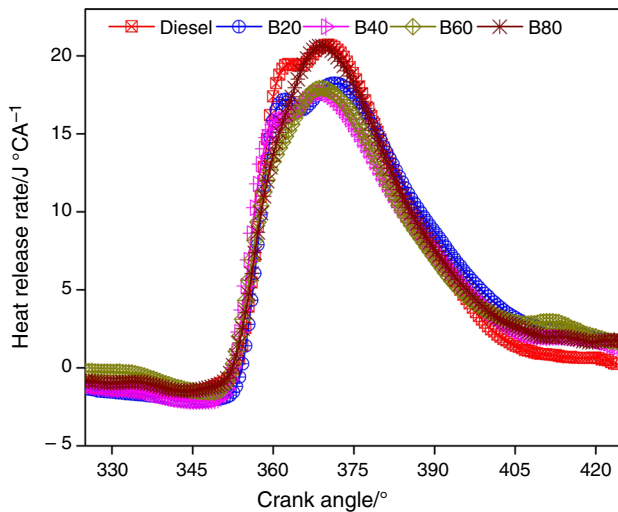

Fig. 10 Variations in heat release rate with blends under supercharging of 0.25 bar (g) at CR 20

Fig. 11. An increase in air boost pressure at inlet enhanced the heat release rate the later stage of combustion. The lower heating value of biodiesel decreases the heat release rate of biodiesel compared to that of diesel [36].

Ignition delay (ID)

Ignition delay of diesel engine is predicted by an empirical formula developed by Hardenberg and Hase [37, 38] to give good agreement with experimental data over wide range of operating conditions as
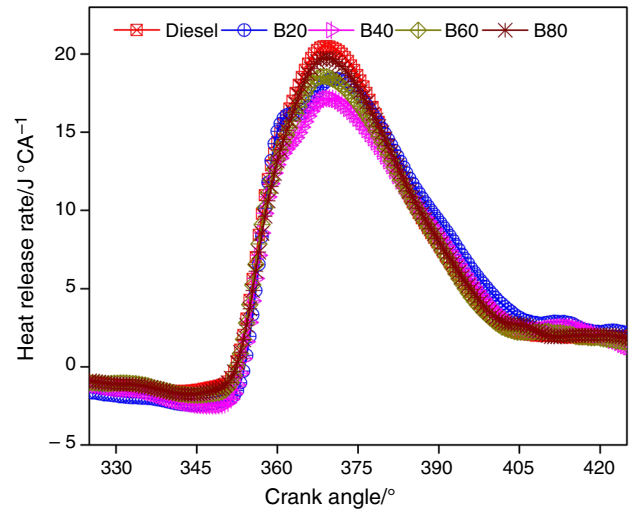
Fig. 11 Variations in heat release rate with blends under supercharging of 0. 5 bar (g) at CR 20

$$\tau_{id(CA)} = (0.36 + 0.22 U_p)$$
$$\exp\left[E_A \left(\frac{1}{\bar{R}T} - \frac{1}{17,190} \right) \left(\frac{21.2}{(p - 12.4)} \right)^{0.63} \right] \quad (9)$$

Mean piston speed, $U_p = 2SN$

where S stroke, N speed in rpm.

Apparaent activation energy, $E_A = 618840/(CN + 25)$

where $\bar{R}$ universal gas constant, p charge pressure, T charge temperature, U_p mean piston speed, CN cetane index and E_A apparent activation energy, which were taken from experimental data.

Normally, biodiesel had shorter ignition delay due to its oxygen content present in the biodiesel and its high cetane index. But the cetane index of methyl esters of rubber seed oil is less than diesel, which increases the delay period further. Ignition delay is inversely proportional to cetane index [39]. However, increase in CR and supercharging reduces the ignition delay significantly. The results revealed that rise in compression ratio, injection pressure and load reduced the ignition delay presented in Fig. 12. The effect of supercharging at higher compression ratio and at full-load operation reduces the delay period [40] except at supercharging pressure of 0.5 bar (g) at higher compression ratio. The minimum ignition delay obtained for MRSO40 at CR 20 at 160 bar injection pressure without supercharging was 11.4°CA bTDC. There is a rise in ignition delay at CR 20 with supercharging pressure, but at the same time increase in compression ratio without and with supercharging of 0.5 bar(g) reduces the ignition delay significantly with premixed combustion at higher compression ratio [31].
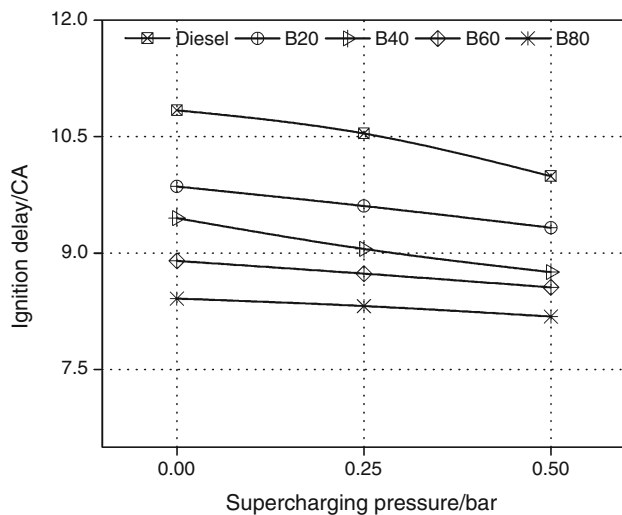
Fig. 12 Variations in ignition delay with supercharging for different blends at CR 20

Fig. 13 Variations in CO emission with supercharging for different blends at CR 20

Emission characteristics

CO emission

An insufficient air in engine cylinder leads to the formation of CO emission. An increase in compression ratio, load and biodiesel blends increases the carbon monoxide emission [15]. At the same time, the result of increase in injection pressure with supercharging provides the sufficient air for better mixing and combustion of fuel reduces the CO emission. The results revealed that the effect of supercharging decreases the CO emission [17]. Figure 13 shows the CO emission with biodiesel blends and supercharging. Higher viscosity of fuel at low and medium loads without supercharging increased the CO emission of higher blends of biodiesel [41]. It is observed that the effect of supercharging lowered the emission of biodiesel blends of MRSO 20, MRSO 40 and diesel owing to its improved air circulation resulting in better cone spray formation of fuel [42].

HC emission

Unburned hydrocarbon emission resulted in improper mixing, insufficient air supply and poor fuel spray formation. A higher blend of biodiesel leads to poor atomization at higher CR, with and without supercharging and increases the HC emission [15]. The effect of supercharging on biodiesel blends of hydrocarbon emission is shown in Fig. 14. There is a decrease in HC emission obtained with increase in airflow of all fuel blends of supercharging compared to naturally aspirated engine [43].
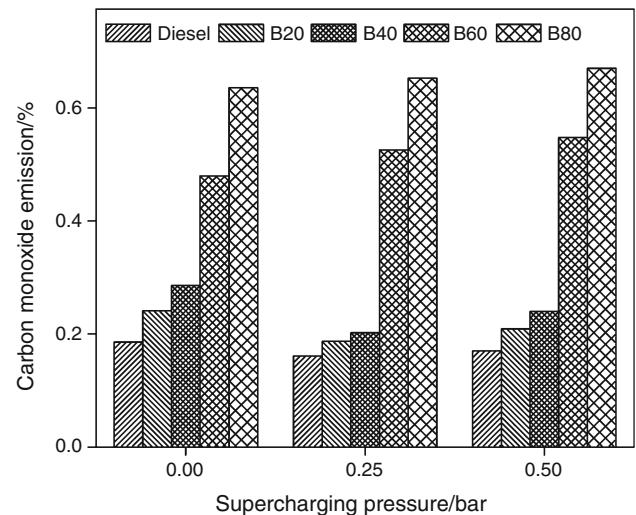

Fig. 14 Variations in HC emission with supercharging for different blends at CR 20
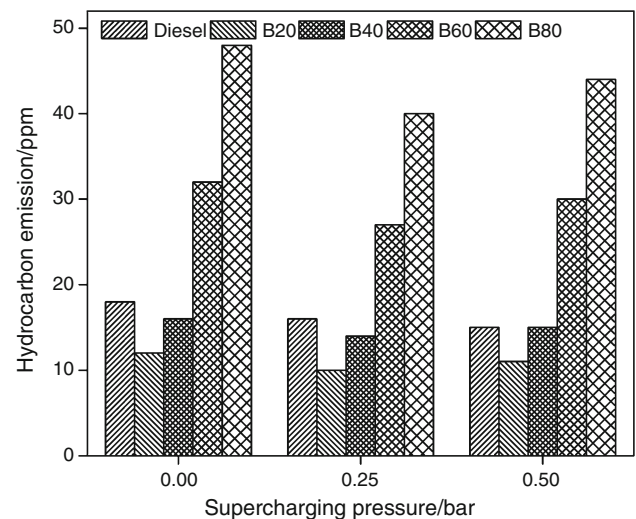
CO$_2$ emission

The CO$_2$ emission is increased with supercharging compared to naturally aspirated engine [44] due to its better combustion. The emission is observed at full-load condition at a CR of 20 with different fuel blends and supercharging pressures as shown in Fig. 15. The increase in biodiesel content increased the CO$_2$ emission [45] with supercharging of all blends except MRSO 40 at 0.25 bar (g) pressure. Sufficient air inside the engine cylinder improves the atomization of fuel blends, and oxygen present in the biodiesel enhances the combustion [43].
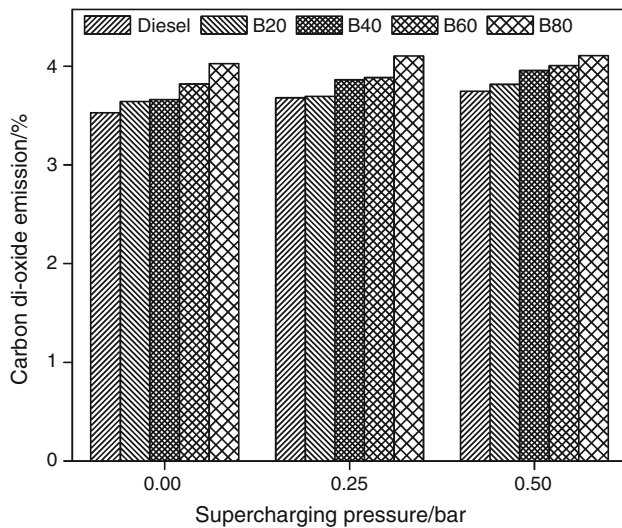
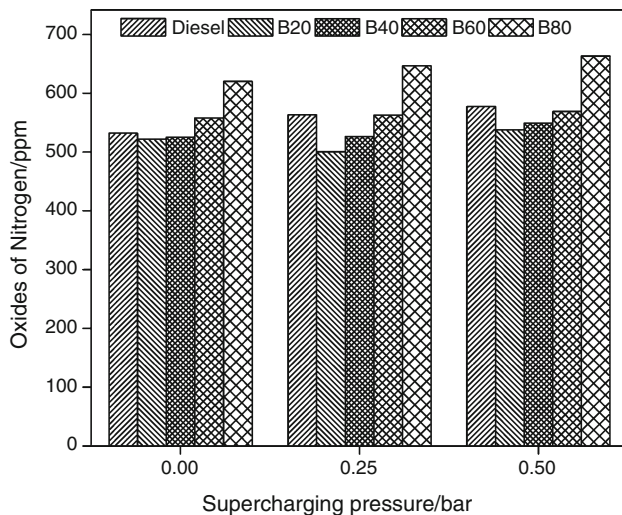**Fig. 15** Variations in CO_2 emission with supercharging for different blends at CR 20

Fig. 16 Variations in NO_x emission with supercharging for different blends at CR 20

NO_x emission

The NO_x emission resulted in the dissociation of nitrogen atom in air at high temperature inside the cylinder above 2000 °C. The combustion of biodiesel in diesel engine increases the in-cylinder temperature due to its oxygen content present in the fuel and shorter ignition delay [17]. It is observed that the variation in CR and injection pressure at part and full-load operation of lower biodiesel blends with supercharging [16] reduces the residence time [46] and prevents sudden rise in cylinder temperature. The NO_x emission is reduced for all blends with supercharging as shown in Fig. 16, except for MRSO 60 and MRSO 80 due to its higher viscosity and poor mixture formation [13, 14].

The results revealed that there is an increase in NO_x emission observed for all fuel blends except diesel in NA condition [15]. The main aim of the research is to reduce the NO_x emission with the help of supercharging in par with CR. The NO_x reduction found to be at 0.25 bar (g) for diesel and MRSO 40 is 562 ppm and 437 ppm, respectively.

Conclusions

The performance, emission and combustion characteristics of VCR engine fueled with MSRO are analyzed effectively by treating CR, load, biodiesel blends, injection pressure and supercharging as operating parameters. The effect of supercharging with lower blends at optimum compression ratio increases the performance parameters and combustion pressure. The emission of CO and HC is reduced significantly using rubber seed oil methyl ester at this CR with supercharging.

The RSM is used effectively to form the empirical relation to predict the responses. The desirability-based optimality is chosen to optimize the factors for each response. The results of optimized parameters MRSO 20, CR 20, supercharging pressure 0.25 (g) bar, 8 kg load, injection pressure 160 bar are obtained from the D-optimality. The results of D-optimality are also tested in VCR engine and are found to be close to each other compared with the experimental results. The overall desirability achieved is 0.98548 and for the responses which are acceptable ones.

When the optimized parameters are implemented in the VCR engine, there is a decrease in CO emission and HC emission of 13.4% and 20% compared with diesel. The NO_x emission is close [14] to diesel due to its optimum CR, IP and reduced residence time of combustion air [47]. The maximum pressure and ID of diesel were 0.12% and 5.54% less than that of MRSO20. Exhaust gas temperature of blend 20 is 10.87% higher than diesel due to its shorter ID [30]. The BTE of MRSO20 was 8.43% higher than diesel with a reduction in fuel consumption of 11.2%.

Once the biodiesel content in the fuel is increased to MRSO40 with same input parameters, NO_x emission is decreased by 9.22% compared to diesel with the supply of combustion air that prevents sudden rise in cylinder temperature [46]. Also, CO and HC emissions are decreased by 22.4% and 12%, respectively, compared to diesel. The heat release rate of biodiesel is improved with inlet air boost pressure compared to that of diesel. Maximum pressure and ID are increased by 4.71% and 0.42% compared to diesel due to its energy content of biodiesel and shorter ID of biodiesel. However, the BTE of MRSO40 was 6.49%

higher than diesel with a decrease in fuel consumption of 1.16% due to its better lubricity of biodiesel.

This study aimed to increase CR at stationary diesel engine to utilize the biodiesel available in rural centers. These works suggest that the use of rubber seed oil blends up to 40% in a VCR engine for agricultural sectors in and around southern districts of Tamil Nadu in India to improve the performance with lower emissions.

References

1. Tompkins BT, Song H, Bittle JA, Jacobs TJ. Efficiency considerations for the use of blended biofuel in diesel engines. Appl Energy. 2012;98:209–18.
2. Godiganur S, Murthy CS, Reddy RP. 6BTA 5.9 G2-1 cummins engine performance and emission tests using methyl ester mahua (Madhuca indica) oil/diesel blends. Renew Energy. 2009;34(10):2172–7.
3. Grau B, Bernat E, Rita P, Jordi-Roger R, Antoni R. Environmental life cycle assessment of rapeseed straight vegetable oil as self-supply agricultural biofuel. Renew Energy. 2013;50:142–9.
4. Kapilan N, Babu TA, Reddy RP. Characterization and effect of using Mahua oil biodiesel as fuel in compression ignition engine. J Therm Sci. 2009;18(4):382–4.
5. Wu X, Daniel R, Tian G, Xu H, Huang Z, Richardson D. Dual-injection: the flexible, bi-fuel concept for spark-ignition engines fuelled with various gasoline and biofuel blends. Appl Energy. 2011;88(7):2305–14.
6. Atabani AE, Silitonga AS, Ong HC, Mahlia TMI, Masjuki HH, Badruddin IA, Fayaz H. Non-edible vegetable oils: a critical evaluation of oil extraction, fatty acid compositions, biodiesel production, characteristics, engine performance and emissions production. Renew Sustain Energy Rev. 2013;18:211–45.
7. Lujaji F, Bereczky A, Janosi L, Novak C, Mbarawa M. Cetane number and thermal properties of vegetable oil, biodiesel, 1-butanol and diesel blends. J Therm Anal Calorim. 2010;102(3):1175–81.
8. Ramadhas AS, Jayaraj S, Muraleedharan C. Biodiesel production from high FFA rubber seed oil. Fuel. 2005;84(4):335–40.
9. Gimbun J, Ali S, Kanwal CCSC, Shah LA, Muhamad NH, Cheng CK, Nurdin S. Biodiesel production from rubber seed oil using activated cement clinker as catalyst. Proc Eng. 2013;53:13–9.
10. Kumar SS, Purushothaman K. High FFA rubber seed oil as an alternative fuel for diesel engine—an overview. Int J Eng Sci. 2012;1(10):16–24.
11. Devi VM, Prasad PN, Syndia LAM, Rajakohila M, Ariharan VN. Physico-chemical characterization of rubber seed oil (Hevea Brasiliensis)—a promising feedstock for biodiesel production. Int J Chem Anal Sci. 2012;3(5):1402–4.
12. Gopinath A, Sairam K, Velraj R. A review on combustion, performance, and emission characteristics of fuels derived from oil seed crops (biodiesels). Aus J Crop Sci. 2013;7(9):1350–4.
13. Ramadhas AS, Jayaraj S, Muraleedharan C. Characterization and effect of using rubber seed oil as fuel in the compression ignition engines. Renew Energy. 2005;30(5):795–803.
14. Pradeep V, and RP Sharma. Evaluation of performance, emission and combustion parameters of a CI engine fuelled with bio-diesel from rubber seed oil and its blends. SAE paper no. 200526353 (2005).
15. Geo VE, Nagarajan G, Nagalingam B. Studies on improving the performance of rubber seed oil fuel for diesel engine with DEE port injection. Fuel. 2010;89(11):3559–67.
16. Rao GAP, Mohan PR. Effect of supercharging on the performance of a DI diesel engine with cotton seed oil. Energy Convers Manag. 2003;44(6):937–44.
17. Jagadish D, Kumar PR, Murthy KM. The effect of supercharging on performance and emission characteristics of compresion ignition engine with diesel-ethanol-ester blends. Therm Sci. 2011;15(4):1165–74.
18. Singh N, Kumar H, Jha MK, Sarma AK. Complete heat balance, performance, and emission evaluation of a CI engine fueled with Mesua ferrea methyl and ethyl ester's blends with petrodiesel. J Therm Anal Calorim. 2015;122(2):907–16.
19. Ebrahimi R, Sherafati M. Thermodynamic simulation of performance of a dual cycle with stroke length and volumetric efficiency. J Therm Anal Calorim. 2013;111(1):951–7.
20. Ebrahimi R, Dehkordi NS. Effects of design and operating parameters on entropy generation of a dual cycle. J Therm Anal Calorim. 2018;133(3):1609–16.
21. Sivaramakrishnan K, Ravikumar P. Optimization of operational parameters on performance and emissions of a diesel engine using biodiesel. Int J Environ Sci Technol. 2014;11(4):949–58.
22. Bharadwaz YD, Rao BG, Rao VD, Anusha C. Improvement of biodiesel methanol blend performance in a variable compression ratio engine using response surface methodology. Alexa Eng J. 2016;55(2):1201–9.
23. Murugapoopathi S, and D Vasudevan. Energy and exergy analysis on variable compression ratio multi-fuel engine. J Therm Anal Calorim, 2018: 1-12.
24. Ramadhas AS, Muraleedharan C, Jayaraj S. Performance and emission evaluation of a diesel engine fueled with methyl esters of rubber seed oil. Renew energy. 2005;30(12):1789–800.
25. Maurya RK, Agarwal AK. Experimental investigation on the effect of intake air temperature and air–fuel ratio on cycle-to-cycle variations of HCCI combustion and performance parameters. Appl Energ. 2011;88(4):1153–63.
26. Cox DD, Snell EJ. The analysis of binary data. 2nd ed. London: Chapman and Hall; 1989.
27. Montgomery DC, Myers RH. Response surface methodology. In: Design and analysis of experiments. 1995. pp. 445–74.
28. Wilson VH. Optimization of diesel engine parameters using Taguchi method and design of evolution. J Bras Soc Mech Sci Eng. 2012;34(4):423–8.
29. Muralidharan K, Vasudevan D. Performance, emission and combustion characteristics of a variable compression ratio engine using methyl esters of waste cooking oil and diesel blends. Appl Energy. 2011;88(11):3959–68.
30. Kannan GR, Anand R. Experimental investigation on diesel engine with diestrol–water micro emulsions. Energy. 2011;36(3):1680–7.
31. Muralidharan K, Vasudevan D, Sheeba KN. Performance, emission and combustion characteristics of biodiesel fuelled variable compression ratio engine. Energy. 2011;36(8):5385–93.
32. VenkateswaraRao B, Rao GAP. Prediction of heat-release patterns for modeling diesel engine performance and emissions. Int J Adv Eng Tech. 2012;3(1):262–9.
33. Planells RC, Amengual AC, Larruy AC. Motores de combustión interna—Fundamentos. Barcelona: Edicions UPC; 1995.

34. Vinukumar K, Azhagurajan A, Vettivel SC, Vedaraman N. Rice husk as nanoadditive in diesel–biodiesel fuel blends used in diesel engine. J Therm Anal Calorim. 2018;131(2):1333–43.

35. Bora BJ, Saha UK. Experimental evaluation of a rice bran biodiesel–biogas run dual fuel diesel engine at varying compression ratios. Renew Energy. 2016;87:782–90.

36. Andrade RD, Faria EA, Silva AM, Araujo WC, Jaime GC, Costa KP, Prado AG. Heat of combustion of biofuels mixed with fossil diesel oil. J Therm Anal Calorim. 2011;106(2):469–74.

37. Hardenberg HO, & Hase FW. An empirical formula for computing the pressure rise delay of a fuel from its cetane number and from the relevant parameters of direct-injection diesel engines. SAE paper no. 790493 (1979).

38. Heywood JB. Internal combustion engine fundamentals. New York: McGraw-Hill Intern. Editions; 1988.

39. Saravanan S, Nagarajan G, Rao GLN, Sampath S. Combustion characteristics of a stationary diesel engine fuelled with a blend of crude rice bran oil methyl ester and diesel. Energy. 2010;35(1):94–100.

40. Paul G, Datta A, Mandal BK. An experimental and numerical investigation of the performance, combustion and emission characteristics of a diesel engine fueled with Jatropha biodiesel. Energy Proc. 2014;54:455–67.

41. Raheman H, Jena PC, Jadav SS. Performance of a diesel engine with blends of biodiesel (from a mixture of oils) and high-speed diesel. Int J Energy Environ Eng. 2013;4(1):6.

42. Tamilvanan A, Balamurugan K, Vijayakumar M. Effects of nano-copper additive on performance, combustion and emission characteristics of Calophyllum inophyllum biodiesel in CI engine. J Therm Anal Calorim. 2018;136:1–14.

43. Reshad AS, Barman P, Chaudhari AJ, Tiwari P, Kulkarni V, Goud VV, Sahoo N. Rubber seed oil methyl ester synthesis, engine performance, and emission characteristics of blends. Energy Fuels. 2015;29(8):5136–44.

44. Ramadhas AS, Jayaraj S, Muraleedharan C. Dual fuel mode operation in diesel engines using renewable fuels: rubber seed oil and coir-pith producer gas. Renew Energy. 2008;33(9):2077–83.

45. Reksowardojo IK, Bui HN, Sok R, Kilgour AJ, Brodjonegoro TP, Soerawidjaja TH, Arismunandar W. The effect of biodiesel fuel from rubber (Hevea brasiliensis) seed oil on a direct injection (DI) diesel engine. Bandung Inst Teknologi Bandung. 2011;1(1):65–81.

46. Vallinayagam R, Vedharaj S, Yang WM, Lee PS. Operation of neat pine oil biofuel in a diesel engine by providing ignition assistance. Energy Convers Manag. 2014;88:1032–40.

47. Clean Air Technology Center. (1999). Nitrogen oxides (NO$_x$): why and how they are controlled.

Publisher's Note Springer Nature remains neutral with regard to jurisdictional claims in published maps and institutional affiliations.